

Chemical Structure and Properties of Interstrand Cross-Links Formed by Reaction of Guanine Residues with Abasic Sites in Duplex DNA

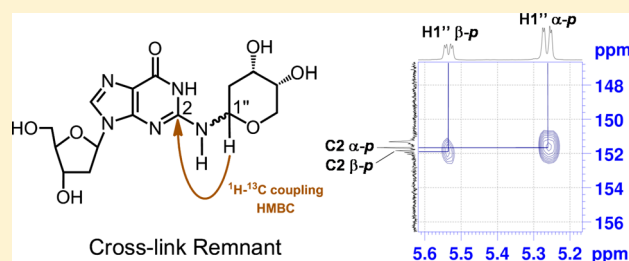
Michael J. Catalano,[†] Shuo Liu,[‡] Nisana Andersen,[‡] Zhiyu Yang,[†] Kevin M. Johnson,[†] Nathan E. Price,[†] Yinsheng Wang,[‡] and Kent S. Gates^{*,†,§}

[†]Department of Chemistry and [§]Department of Biochemistry, University of Missouri, 125 Chemistry Building, Columbia, Missouri 65211, United States

[‡]Environmental Toxicology Graduate Program and Department of Chemistry, University of California—Riverside, Riverside, California 92521-0403, United States

S Supporting Information

ABSTRACT: A new type of interstrand cross-link resulting from the reaction of a DNA abasic site with a guanine residue on the opposing strand of the double helix was recently identified, but the chemical connectivity of the cross-link was not rigorously established. The work described here was designed to characterize the chemical structure and properties of dG–AP cross-links generated in duplex DNA. The approach involved characterization of the nucleoside cross-link “remnant” released by enzymatic digestion of DNA duplexes containing the dG–AP cross-link. We first carried out a chemical synthesis and complete spectroscopic structure determination of the putative cross-link remnant **9b** composed of a 2-deoxyribose adduct attached to the exocyclic *N*²-amino group of dG. A reduced analogue of the cross-link remnant was also prepared (**11b**). Liquid chromatography–tandem mass spectrometric (LC-MS/MS) analysis revealed that the retention times and mass spectral properties of synthetic standards **9b** and **11b** matched those of the authentic cross-link remnants released by enzymatic digestion of duplexes containing the native and reduced dG–AP cross-link, respectively. These results establish the chemical connectivity of the dG–AP cross-link released from duplex DNA and provide a foundation for detection of this lesion in biological samples. The dG–AP cross-link in duplex DNA was remarkably stable, decomposing with a half-life of 22 days at pH 7 and 23 °C. The intrinsic chemical stability of the dG–AP cross-link suggests that this lesion in duplex DNA may have the power to block DNA-processing enzymes involved in transcription and replication.



INTRODUCTION

Many molecules that contain an aldehyde functional group display mutagenic or cytotoxic properties that stem from their ability to covalently modify DNA.^{1–17} Reversible attack of DNA nucleophiles on the electrophilic aldehyde carbon typically yields an equilibrating mixture of hemiaminal and imine adducts (**1** and **2**, Scheme 1).^{1,4–14} In some cases, aldehyde–DNA adducts have been stabilized for analysis via irreversible reduction of iminium ion **3** to amine **4** by use of reagents such as NaCNBH₃ under mildly acidic conditions (Scheme 1).^{4,18–20}

We recently identified a special class of aldehyde–DNA adducts derived from the reaction of DNA abasic (AP) sites with nucleobases on the opposing strand of the double helix.^{21–23} AP sites are prevalent lesions in genomic DNA that are generated by a wide variety of endogenous cellular processes,^{24–28} drugs,²⁵ bioactive natural products,^{29–34} and environmental carcinogens.^{25,26} AP sites exist as an equilibrium mixture of the ring-closed hemiacetal **5** and the ring-opened aldehyde **6** (Scheme 2).³⁵ We showed that the AP-aldehyde can react reversibly with guanine or adenine residues on the opposing strand of the double helix to generate DNA–DNA

interstrand cross-links (Scheme 3).^{21–23} In the case of the dG–AP cross-link, treatment with NaCNBH₃ generated a reduced, chemically stable analogue of the cross-link.²¹ Interstrand cross-links are extremely deleterious because they block replication and transcription and present serious challenges to cellular DNA repair systems.^{36–39} Accordingly, AP-derived cross-links have the potential to contribute to aging, sporadic cancers, and biological effects of the various xenobiotics that induce AP sites in cellular DNA.^{36–40}

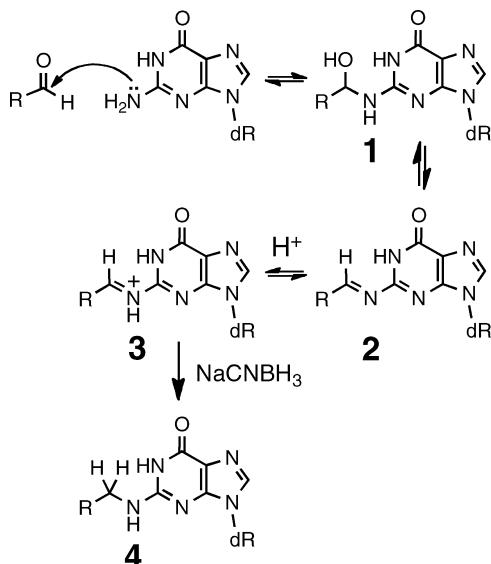
In earlier work, we proposed that dG–AP cross-linking involves attachment of the exocyclic *N*²-amino group of dG to the anomeric carbon of the AP residue (Scheme 3), but the chemical connectivity of the cross-link was not rigorously determined.^{21,22} For example, we recognized that the biochemical and mass spectrometric data could not rule out cross-link structures involving attachment of the AP-aldehyde at an endocyclic nitrogen of dG or conversion of an initial imine adduct to the enamine **10a**.

Complete understanding of the molecular events underlying the biological consequences of any given DNA lesion requires

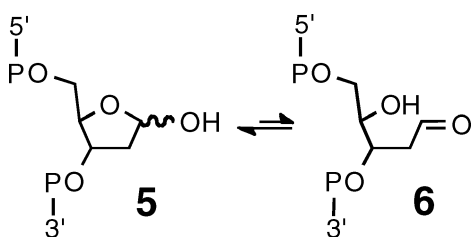
Received: January 20, 2015

Published: February 24, 2015

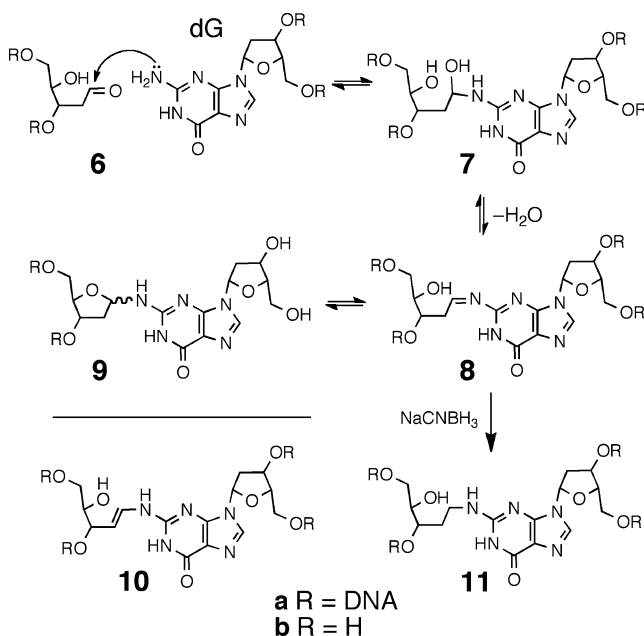
Scheme 1



Scheme 2



Scheme 3



precise knowledge of chemical structure. Chemical structure determination of a DNA lesion, in turn, requires full spectroscopic characterizations of the lesion.⁴¹ The results described here were designed to shed light on the chemical structure and properties of dG-AP cross-links generated in duplex DNA.

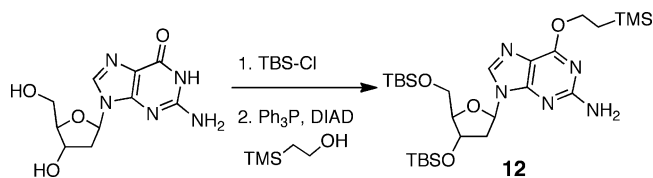
Toward this end, we characterized the nucleoside cross-link “remnant” released by enzymatic digestion of a DNA duplex containing the dG-AP cross-link.²¹ We first carried out a chemical synthesis and complete spectroscopic structure determination of the putative nucleoside cross-link remnant **9b**. Liquid chromatography–tandem mass spectrometry (LC-MS/MS) analysis was then used to demonstrate that the properties of the authentic cross-link remnant released by enzymatic digestion of a DNA duplex containing the dG-AP cross-link matched those of the synthetic material **9b**. The reduced cross-link **11** (Scheme 3) was similarly characterized. The results establish the chemical connectivity of the dG-AP cross-link released from duplex DNA and provide a foundation for detection of this lesion in biological samples. The cross-link remnant **9b** was quite stable, decomposing to release dG with a half-life of approximately 17 days at pH 7 and 23 °C. NMR spectroscopic data suggests that the stability of this material is due to the fact that the 2-deoxyribose adduct connected at the N²-position of dG exists as a mixture of the ring-closed α -pyranose, β -pyranose, α -furanose, and β -furanose isomers, with no detectable amounts of the hydrolytically labile imine present (**9b**, Scheme 5). The intrinsic stability of the cross-link attachment observed in the nucleoside remnant was mirrored in the stability of the actual cross-link in duplex DNA, which dissociated with a half-life of 22 days at pH 7 and 23 °C. This suggests that the dG-AP cross-link may have the power to block critical DNA-processing enzymes.

EXPERIMENTAL PROCEDURES

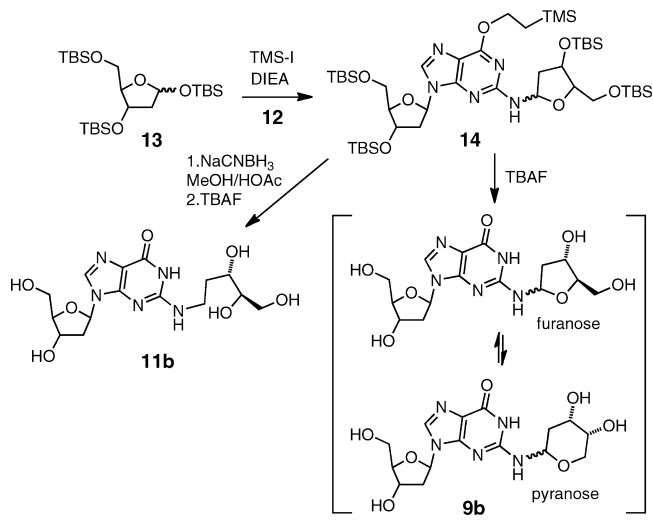
Materials and Methods. Oligonucleotides were purchased from Integrated DNA Technologies (Coralville, IA). Uracil-DNA glycosylase (UDG, 5000 units/mL) and UDG buffer were purchased from New England Biolabs (Ipswich, MA). 2'-Deoxyguanosine (dG) monohydrate was purchased from Tokyo Chemical Industry Co., Ltd. (Tokyo, Japan). 2-Deoxy-D-ribose (99%), *N,N*-diisopropylethylamine (redistilled, 99.5%), and tetrabutylammonium fluoride (1 M in tetrahydrofuran, THF) were purchased from Sigma-Aldrich (St. Louis, MO). Iodotrimethylsilane (97%) was purchased from Acros Organics (Thermo Fisher) in a 5 g vial and stored at -15 °C in a desiccator; a small amount of metallic copper was added to the vial as a stabilizer. All other reagents used were purchased from Acros Organics in reagent grade and used without further purification unless otherwise noted. Bulk solvents (hexanes, ethyl acetate, and CH₂Cl₂) were obtained from Sigma-Aldrich. Methanol, THF, and H₂O were purchased from Fisher in HPLC grade. When used as reaction solvents, CH₂Cl₂ and methanol were dried over 4 and 3 Å molecular sieves, respectively. THF was distilled prior to use. Anhydrous *N,N*-dimethylformamide (DMF) and dioxane were purchased in AcroSeal bottles from Acros Organics. Column chromatography was performed on silica gel 60 (Sigma-Aldrich) under positive pressure. Glass-backed thin-layer chromatography (TLC) plates with a 254 nm fluorescent indicator were purchased from Sigma-Aldrich and stored in a desiccator. Compounds on developed TLC plates were visualized by use of a 254 nm UV lamp or by dipping in a solution of 10% phosphomolybdic acid hydrate (PMA) in ethanol solution, followed by charring with a heat gun. Unless otherwise specified, reactions were conducted under an atmosphere of dry N₂ gas. ¹H and ¹³C NMR spectra were recorded on a Bruker DRX500 at 298 K in CDCl₃, deuterated dimethyl sulfoxide (DMSO-*d*₆), or D₂O (Cambridge Isotope Laboratories, Inc.).

Syntheses. *O*⁶-(Trimethylsilyl)ethyl-3',5'-bis[*O*-(*tert*-butyldimethylsilyl)]-2'-deoxyguanosine (**12**). To a solution containing triphenylphosphine (1.91 g, 7.28 mmol) and 2-(trimethylsilyl)ethanol (1.04 mL, 7.28 mmol) in dry dioxane (12 mL) was added 3',5'-bis-*O*-(*tert*-butyldimethylsilyl)-2'-deoxyguanosine (1.44 g, 2.91 mmol), which was prepared as described previously.⁴² Diisopropylazodicarboxylate (1.43 mL, 7.28 mmol) was added slowly by syringe, causing

Scheme 4



Scheme 5



the white slurry to turn translucent yellow upon complete addition. After stirring for 2 h at 23 °C, the solvent was evaporated and the crude oil was redissolved in diethyl ether (12 mL). Triphenylphosphine oxide was crystallized from the mixture by submersion of the flask in liquid N₂ and then removed by vacuum filtration. The filtrate was concentrated to a yellow oil and column chromatography on silica gel, eluted with 5:1 hexane/ethyl acetate, gave **12** (1.18 g, 68%, *R_f* = 0.21 5:1 hexane/ethyl acetate) as a sticky yellow solid: ¹H NMR (500 MHz, CDCl₃) δ 7.86 (1H, s, H8), 6.30 (1H, t, *J* = 6.5 Hz, H1'), 4.92 (2H, br s, NH₂), 4.59–4.56 (1H, m, H3'), 4.56–4.52 (2H, m, ROCH₂CH₂TMS), 3.96 (1H, q, *J* = 3.5 Hz, H4'), 3.79 (1H, dd, *J* = 4.5, 11 Hz, H5a'), 3.73 (1H, dd, *J* = 3.3, 11.3 Hz, H5b'), 2.55 (1H, dt, *J* = 6.5, 13.3 Hz, H2a'), 2.33 (1H, ddd, *J* = 3.5, 6, 13 Hz, H2b'), 1.24–1.19 (2H, m, ROCH₂CH₂TMS), 1.00–0.77 [18H, m, Si(CH₃)₃], 0.08 [6H, s, Si(CH₃)₂], 0.06 [6H, s, ROEtSi(CH₃)₃], 0.06 [3H, s, ROEtSi(CH₃)₃], 0.05 [6H, s, Si(CH₃)₂]; ¹³C NMR (126 MHz, CDCl₃) δ 161.3 (C6), 159.2 (C2), 153.3 (C4), 137.3 (C8), 115.9 (C5), 87.6 (C4'), 83.5 (C1'), 71.9 (C3'), 64.8 (ROCH₂CH₂TMS), 62.8 (C5'), 40.8 (C2'), 25.9, 25.7 [Si(CH₃)₃], 18.4, 18.0 [Si(CH₃)₃], 17.5 (ROCH₂CH₂TMS), -1.5 [ROEtSi(CH₃)₃], -4.7, -4.8, -5.4, -5.6 [Si(CH₃)₂].

1,3,5-Tris[O-(tert-butyl dimethylsilyl)]-2-deoxy-D-ribofuranose (13). 2-Deoxy-D-ribose (1.50 g, 11.18 mmol), *tert*-butyldimethylsilyl chloride (5.60 g, 37.16 mmol), and imidazole (3.00 g, 44.07 mmol) were dissolved in anhydrous DMF (15 mL) and stirred at 23 °C. After 19 h, the reaction mixture was diluted with hexane (100 mL), washed with water (3 × 50 mL) and brine (1 × 50 mL), and dried over Na₂SO₄, and the solvent was evaporated under reduced pressure to give a light yellow oil. Column chromatography on silica gel, eluted with 3% ethyl acetate in hexane, gave **13** (3.83 g, 72%) as a colorless gel (*R_f* = 0.37 in 3% ethyl acetate–hexane): ¹H NMR (500 MHz, CDCl₃, α and β = anomeric isomers, p and f = pyranose and furanose isomers) δ 5.60 (0.40H, t, *J* = 4.3 Hz, H1 β-f), 5.46 (0.37H, dd, *J* = 2.5, 5 Hz, H1 α-f), 5.20 (0.21H, dd, *J* = 2.3, 5 Hz, H1 β-p), 4.75 (0.02H, dd, *J* = 2.5, 7.5 Hz, H1 α-p), 4.36 (0.40H, dt, *J* = 3.2, 5.1 Hz, H3 β-f), 4.18 (0.37H, dt, *J* = 4.8, 7.8 Hz, H3 α-f), 4.14–4.10 (0.02H, m, H3 α-p), 4.09–4.05 (0.21H, m, H3 β-p), 3.97 (0.37H, q, *J* = 4.3 Hz, H4 α-f), 3.89–3.86 (0.02H, m, H4 α-p), 3.84 (0.40H, ddd, *J* = 3, 5,

7.5 Hz, H4 β-f), 3.75–3.69 (0.42H, m, H4 and H5a β-p), 3.67–3.59 (1.37H, m, H5a β-f, H5 α-f, H5b β-p, and H5a α-p), 3.57 (0.40H, dd, *J* = 7.5, 10.5 Hz, H5b β-f), 3.31 (0.02H, dd, *J* = 1.5, 12 Hz, H5b α-p), 2.22 (0.37H, ddd, *J* = 5.4, 7.6, 13.1 Hz, H2a α-f), 2.05–1.97 (1H, m, H2 β-f and H2a β-p), 1.97–1.92 (0.02H, m, H2a α-p), 1.82 (0.37H, ddd, *J* = 2.4, 4.4, 13.1 Hz, H2b α-f), 1.72–1.68 (0.02H, m, H2b α-p), 1.58 (0.21H, ddd, *J* = 3.5, 5, 12.5 Hz, H2b β-p), 0.93–0.85 [27H, m, Si(CH₃)₃], 0.11–0.03 [18H, m, Si(CH₃)₂]; ¹³C NMR (126 MHz, CDCl₃) δ 99.1 (C1 β-f), 98.5 (C1 α-f), 94.7 (C1 α-p), 93.0 (C1 β-p), 87.0 (C4 β-f), 85.4 (C4 α-f), 73.3 (C3 β-f), 71.9 (C3 α-f), 70.0 (C4 β-p), 69.9 (C4 α-p), 69.4 (C3 α-p), 68.1 (C3 β-p), 65.8 (C5 α-p), 64.8 (C5 β-f), 64.7 (C5 α-f), 63.0 (C5 β-p), 44.6 (C2 β-f), 44.4 (C2 α-f), 38.7 (C2 β-p), 38.5 (C2 α-p), 26.0, 25.9, 25.8, 25.8, 25.7, 25.7 [Si(CH₃)₃], 18.4, 18.3, 18.1, 18.0, 18.0, 17.9, 17.9 [Si(CH₃)₃], -4.1, -4.2, -4.2, -4.4, -4.5, -4.6, -4.7, -4.7, -4.7, -4.8, -4.8 [Si(CH₃)₂].

N²-[3,5-Bis[O-(*tert*-butyldimethylsilyl)]-2-deoxy-D-ribofuranos-1-yl]-O⁶-benzyl-3',5'-bis[O-(*tert*-butyldimethylsilyl)]-2'-deoxyguanosine (14). Compound **13** (248 mg, 0.499 mmol) was dissolved in dry CH₂Cl₂ (2 mL) in an oven-dried round-bottom flask. The flask was purged with dry N₂ and cooled in a -78 °C dry ice–acetone bath. Trimethylsilyl iodide (TMS-I; 71 μL, 0.499 mmol) was added via syringe to generate the glycosyl iodide, and the resulting light yellow liquid was stirred for 10 min. A solution of **12** (50 mg, 0.084 mmol) and diisopropylethylamine (DIPEA, 120 μL, 0.689 mmol) in dry CH₂Cl₂ (250 μL) was added by syringe, and the mixture was stirred for 15 min at -78 °C and then for an additional 15 min while warming to room temperature. Unreacted glycosyl iodide was quenched by the addition of dry MeOH (4 mL). The mixture was evaporated to dryness under reduced pressure, redissolved in 7:1 hexane–ethyl acetate, and washed with H₂O to remove the diisopropylethylammonium hydroiodide salt. The organic layer was dried over Na₂SO₄ and evaporated under reduced pressure to yield a yellow oil. Column chromatography on silica gel, eluted with 7:1 hexane–ethyl acetate (v/v), gave **14** (43 mg, 54%, *R_f* = 0.25) as a white foam: TOF-MS/ES⁺ 940.5687 M⁺; ¹H NMR (500 MHz, CDCl₃) δ 7.86 (0.2H, s, H8 β-f), 7.84 (0.8H, s, H8 α-f), 6.49 (0.8H, d, *J* = 10.5 Hz, NH α-f), 6.37 (0.2H, m, H1'), 6.31 (0.8H, t, *J* = 6.5 Hz, H1'), 6.29–6.26 (0.2H, m, H1' β-f), 6.21 (0.8H, dd, *J* = 6.5, 10.5 Hz, H1' α-f), 5.39 (0.2H, d, *J* = 10 Hz, NH β-f), 4.60–4.55 (1H, m, H3'), 4.55–4.47 (2H, m, OCH₂CH₂TMS), 4.45 (0.8H, d, *J* = 4.5 Hz, H3' α-f), 4.44–4.43 (0.2H, m, H3' β-f), 4.11 (0.8H, dd, *J* = 3.8, 7.3 Hz, H4' α-f), 3.98–3.91 (1H, m, H4'), 3.89 (0.2H, ddd, *J* = 2.4, 2.4, 4.6 Hz, H4' β-f), 3.79 (1H, dd, *J* = 5, 11 Hz, H5a'), 3.75 (1H, dd, *J* = 3.8, 11 Hz, H5b'), 3.72–3.67 (0.2H, m, H5a' β-f), 3.67 (0.8H, dd, *J* = 3.8, 10.8 Hz, H5a' α-f), 3.58 (0.2H, dd, *J* = 5, 10.5 Hz, H5b' β-f), 3.36 (0.8H, dd, *J* = 7.5, 10.5 Hz, H5b' α-f), 2.65–2.49 (1H, m, H2a'), 2.39–2.35 (0.2H, m, H2b' β-f), 2.33 (0.8H, ddd, *J* = 3.9, 6.1, 13.1 Hz, H2b' α-f), 2.27–2.20 (0.8H, m, H2a' α-f), 2.20–2.16 (0.2H, m, H2a' β-f), 1.99–1.95 (0.2H, m, H2b' β-f), 1.93 (0.8H, d, *J* = 13 Hz, H2b' α-f), 1.28–1.18 (2H, m, OCH₂CH₂TMS), 0.98–0.88 [36H, m, Si(CH₃)₃], 0.15–0.04 [33H, m, Si(CH₃)₂ and OEtSi(CH₃)₃]; ¹³C NMR (126 MHz, CDCl₃) δ 161.1 (C6), 157.9, 157.6 (C2), 153.3, 153.0 (C4), 137.5, 137.3 (C8), 116.3, 116.2 (C5), 87.7, 87.5 (C4'), 87.0 (C4' α-f), 86.7 (C4' β-f), 84.1 (C1'), 83.6 (C1''), 83.4 (C1'), 74.5 (C3' α-f), 73.1 (C3' β-f), 72.1 (C3'), 64.4 (OCH₂CH₂TMS), 63.9 (C5' β-f), 63.7 (C5' α-f), 63.0 (C5'), 26.0, 26.0, 25.9, 25.8, 25.8 [Si(CH₃)₃], 18.4, 18.4, 18.3, 18.2, 18.0, 18.0, 17.8, 17.5 [Si(CH₃)₃], 17.5 (OCH₂CH₂TMS), -1.4 [OEtSi(CH₃)₃], -4.7, -4.7, -4.7, -4.8, -4.9, -5.3, -5.4, -5.5, -5.5, -5.5 [Si(CH₃)₂]. NMR analysis indicated the presence of a small amount (<5%) of an inseparable isomer whose spectral data are consistent with the N²-α form of **14**. Under some conditions, native N²-β-2'-deoxyguanosine can isomerize to N²-α and N⁷-α/β forms of dG that are not separable by silica gel chromatography.⁴³ We suspected that the electrophilic TMS-I reagent used here may induce small amounts of such isomerization. This was tested by treating **12** with TMS-I and DIPEA, in the absence of **13**. After 48 h, ¹H NMR of the crude mixture revealed a new singlet downfield of the H8 signal for **12**. Similarly, small singlet peaks downfield of H8 were observed in the ¹H NMR spectra for **14** and **9b**

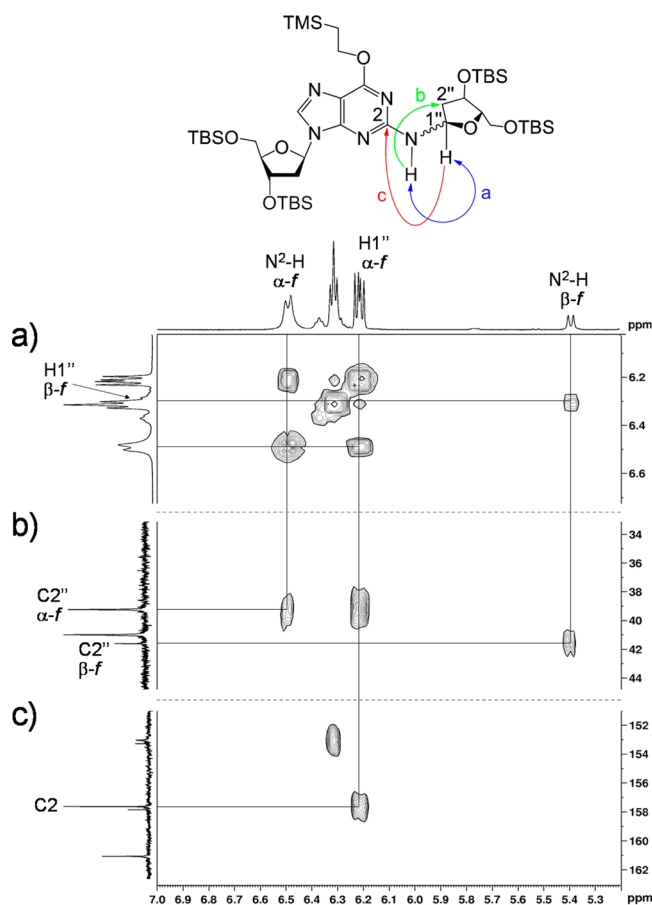


Figure 1. Selected regions of ^1H – ^1H COSY and ^1H – ^{13}C HMBC spectra of **14** in CDCl_3 acquired at 500 (^1H) and 126 (^{13}C) MHz. Attachment of the 3,5-bis[*O*-(*tert*-butyldimethylsilyl)]-2-deoxyribofuranose moiety to N^2 of the protected dG was established by (a) homonuclear (COSY) coupling of $\text{H1}''$ to $\text{N}^2\text{-H}$ as well as three-bond HMBC coupling of (b) $\text{N}^2\text{-H}$ to $\text{C2}''$ and (c) $\text{H1}''$ to C2 .

(Figures S5, S10, and S11, Supporting Information). Additionally, the ^1H NMR spectrum for **11b** contained weak signals whose chemical shifts matched those reported for H8, H3' and H4' of the $\text{N}^9\text{-}\alpha$ isomer of dG.⁴⁴

***N*²-[(3*S*,4*R*)-3,4,5-Trihydroxypentyl]-2'-deoxyguanosine (**11b**).** Compound **14** (48 mg, 0.05 mmol) and NaCNBH_3 (32 mg, 0.51 mmol) were dissolved in a mixture of methanol (2 mL) and acetic acid (6 μL , 0.11 mmol). The solution was stirred at room temperature for 4 h, after which the solvent was removed by rotary evaporation under reduced pressure and the resulting residue redissolved in 10 mL of 7:1 hexane–ethyl acetate (v/v). The organic layer was washed with NaHCO_3 (2 \times 10 mL), H_2O (2 \times 10 mL), and brine (1 \times 10 mL), dried over Na_2SO_4 , and evaporated to give 44 mg of a colorless, sticky oil. This material was dissolved in distilled THF (3 mL) and treated with tetrabutylammonium fluoride (TBAF; 240 μL of a 1 M solution in THF). After 3 h, the mixture was evaporated to give a yellow oil that was redissolved in H_2O (5 mL). Addition of NH_4PF_6 (50 mg, 0.31 mmol) caused precipitation of tetrabutylammonium- PF_6 as a white solid that was removed by extraction with CH_2Cl_2 (4 \times 1.5 mL). This step facilitated purification of **11b** because tetrabutylammonium salts could not otherwise be removed effectively by column chromatography on silica gel. The aqueous layer was evaporated to a white residue that was subjected to column chromatography on silica gel eluted with 15:5:1 $\text{CH}_2\text{Cl}_2/\text{MeOH}/\text{H}_2\text{O}$ (R_f = 0.21) to give **11b** (9 mg, 46%) as a white solid: LC-LTQ-Orbitrap 386.1678 $[\text{M} + \text{H}]^+$; ^1H NMR (500 MHz, D_2O) δ 7.88 (1H, s, H8), 6.25 (1H, t, J = 6.8 Hz, $\text{H1}'$), 4.61 (1H, dt, J = 6.5, 4 Hz, $\text{H3}'$), 4.06 (1H, dt, J = 5.5, 4 Hz, $\text{H4}'$), 3.79 (1H, dd, J = 12.5, 4 Hz,

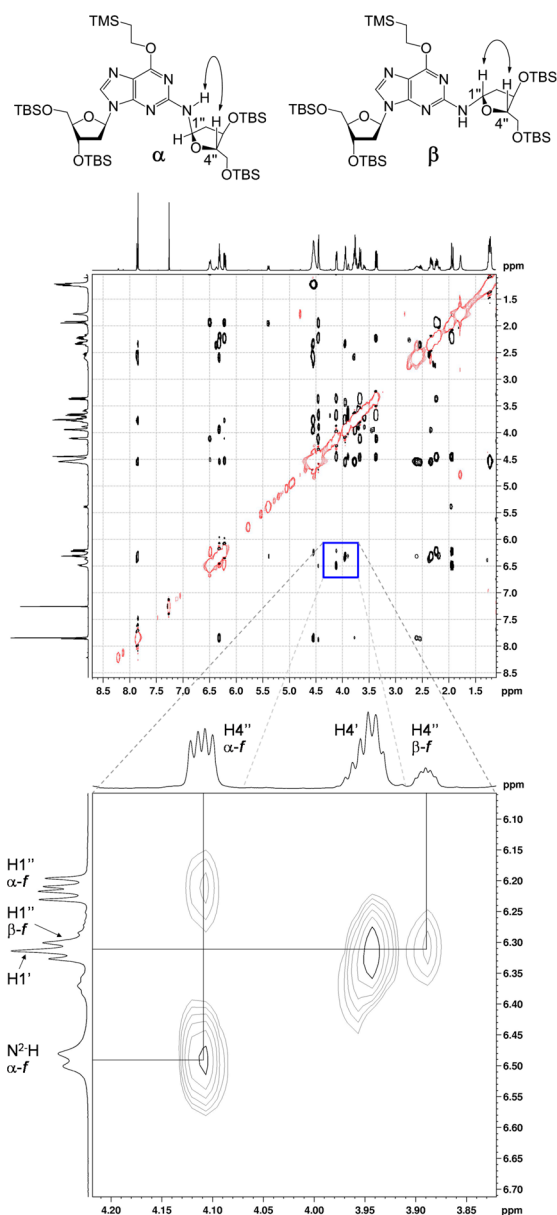
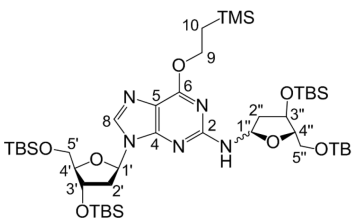


Figure 2. ^1H – ^1H NOESY spectrum of **14** in CDCl_3 acquired at 500 MHz with a mixing time of 800 ms; negative peaks are denoted by red curves. The expanded frame shows the strong through-space correlation between $\text{H4}''$ and $\text{N}^2\text{-H}$ of the major α -furanose isomer. Also shown is a cross-peak between $\text{H4}''$ and $\text{H1}''$ of the minor β -furanose isomer; no correlation between $\text{H4}''$ and $\text{N}^2\text{-H}$ of the minor isomer is evident.

$\text{H5a}'$), 3.74 (1H, dd, J = 12.5, 6.5 Hz, $\text{H5b}'$), 3.73 (1H, dd, J = 18.8, 8.8 Hz, $\text{H5a}''$), 3.71–3.67 (1H, m, $\text{H3}''$), 3.64–3.61 (1H, m, $\text{H4}''$), 3.59 (1H, dd, J = 19.3, 6.8 Hz, $\text{H5b}''$), 3.49–3.44 (2H, m, $\text{H1}''$), 2.86 (1H, dt, J = 13.9, 6.9 Hz, $\text{H2a}'$), 2.47 (1H, ddd, J = 14, 6.5, 4 Hz, $\text{H2b}'$), 2.00–1.91 (1H, m, $\text{H2a}''$), 1.71–1.61 (1H, m, $\text{H2b}''$); ^{13}C NMR (126 MHz, D_2O) δ 159.6 (C6), 153.3 (C2), 152.1 (C4), 116.6 (C5), 138.4 (C8), 87.4 (C4'), 84.5 (C1'), 75.2 (C4''), 71.7 (C3'), 70.1 (C3''), 63.1 (C5''), 62.2 (C5'), 38.7 (C2'), 38.5 (C1''), 32.0 (C2'').

***N*²-[2-Deoxy-D-ribofuran-1-yl]-2'-deoxyguanosine (**9b**).** Compound **14** (88 mg, 0.09 mmol) was dissolved in dry THF (6 mL) and tetrabutylammonium fluoride (562 μL of a 1 M solution in THF) was added by syringe. After the mixture was stirred for 2 h, the solvent was evaporated to give a yellow oil, which was redissolved in H_2O (15 mL). Addition of NH_4PF_6 (120 mg, 0.74 mmol) gave a white precipitate that was removed by extraction with CH_2Cl_2 (4 \times 5 mL). The aqueous

Table 1. Chemical Shifts and 2D Correlations for **14** in CDCl₃


position / isomer	δ_C	H _{a/b}	δ_H (J in Hz)	COSY	TOCSY	HMBC ^a	NOESY
2	157.9, 157.6 ^b						
4	153.3, 153.0						
5	116.3, 116.2						
6	161.1						
8 α	137.5	7.84, s				4, 5	1', 2a', 3, 5a', 5b'
8 β	137.3	7.86, s				4, 5	1', 2a', 3', 5a', 5b'
1' α	84.1	6.31, t (6.5)		2b'	2a', 2b', 3'	4, 8	2a', 2b', 3', 4', 8
1' β	83.4	6.40–6.34, m		2a', 2b'	2a', 2b', 3'	8	2b', 3', 4', 8
2' α	41.0	a 2.67–2.57, m		2b'	1', 2b', 3'		1', 2b', 3', 5a', 5b', 8
		b 2.33, ddd (13.1, 6.1, 3.9)		1', 2a', 3'	1', 2a', 3', 4'	3', 4'	1', 2a', 3', 4'
2' β	(41.0) ^c	a 2.53, ddd (13.4, 6.6, 6.6)		1', 2b', 3'	1', 2b', 3'	1'	
		b 2.39–2.33, m		1', 2a', 3'	1', 2a', 3'	3', 4'	
3'	72.1, 72.1	4.60–4.55, m		2b', 4'	1', 2a', 2b', 4', 5'		1', 2a', 2b', 4', 5a', 5b', 8
4'	87.5	3.98–3.91, m		3', 5'	3', 5'		1', 2b', 3', 5a', 5b'
5'	63.0	a 3.79, dd (11.5)		4'	3', 4'	3'	2a', 3', 4', 8
		b 3.75, dd (11.3, 3.8)		4'	3', 4'	3'	2a', 3', 4', 8
1'' α	83.6	6.21, dd (10.5, 6.5)		2a'', N ² -H	2a'', 2b'', 3'', N ² -H	2, 3'', 4''	2a'', 2b'', 3'', 4''
1'' β	(83.6)	6.29–6.26, m		2a'', 2b'', N ² -H	3''		2a'', 4''
2'' α	39.2	a 2.27–2.20, m		1', 2b'', 3''	1'', 2b'', 3'', N ² -H	2, 1''	1'', 2b'', 3'', 5b''
		b 1.93, d (13)		2a''	1'', 2a'', 3'', N ² -H	3'', 4''	1'', 2a'', 3'', N ² -H
2'' β	41.6	a 2.20–2.16, m		1'', 2b''	2b'', 3'', N ² -H	3'', 4''	1'', 2b'', 3''
		b 1.99–1.95, m		1'', 2a''	2a'', N ² -H	1''	2a'', 3'', N ² -H
3'' α	74.5	4.45, d (4.5)		2a''	1'', 2a'', 2b'', N ² -H	1'', 4'', 5''	1'', 2a'', 2b'', 4'', 5a'', 5b''
3'' β	73.1	4.43, m		2b''	1'', 2a'', 4'', N ² -H		
4'' α	87.0	4.11, dd (7.3, 3.8)		5a'', 5b''	5a'', 5b''	3''	3'', 5a'', 5b'', N ² -H
4'' β	86.7	3.89, ddd (4.6, 2.4, 2.4)		5b''	3'', 5a'', 5b''		
5'' α	63.7	a 3.67, dd (10.8, 3.8)		4'', 5b''	4'', 5b''	3'', 4''	3'', 4'', 5b''
		b 3.36, dd (10.5, 7.5)		4'', 5a''	4'', 5a''	3'', 4''	3'', 4'', 5a''
5'' β	63.9	a 3.72–3.67, m		5b''	4'', 5b''		5b''
		b 3.58, dd (10.5, 5)		5a''	4'', 5a''		5a''
N ² -H α		6.49, d (10.5)		1''	1'', 2a'', 2b'', 3''	2''	2b'', 3'', 4''
N ² -H β		5.39, d (10)		1''	1'', 2a'', 2b''	2''	1'', 2b''
9	64.7, 64.4	4.55–4.47, m		10	10	6	10
10	17.5, 17.5	1.28–1.18, m		9	9	9	9

^aHMBC correlations are from protons in the δ_H column to the listed carbon(s). ^bMultiple ¹³C peaks represent the two stereoisomers of **14**; resonances were assigned to individual isomers where possible. ^cParentheses denote ¹³C signal of the β -isomer is indistinguishable from that of the α -isomer.

layer was evaporated and the resulting white residue was subjected to column chromatography on silica gel, eluted with 15:5:1 MeOH/CH₂Cl₂/H₂O ($R_f = 0.19$), to give **9b** (21 mg, 59%) as an off-white solid: LC-LTQ-Orbitrap 384.1521 [M + H]⁺; ¹H NMR (500 MHz, D₂O) δ 7.94 (1H, br s, H8), 6.35–6.26 (1H, m, H1'), 6.02–6.00 (0.1H, m, H1'' β -f), 6.00–5.98 (0.1H, m, H1'' α -f), 5.54 (0.3H, dd, $J = 8, 2.5$ Hz, H1'' β -p), 5.26 (0.6H, dd, $J = 9.5, 2.5$ Hz, H1'' α -p), 4.67–4.62 (1H, m, H3'), 4.43–4.40 (0.1H, m, H3'' β -f), 4.40–4.37 (0.1H, m, H3'' α -f), 4.22–4.18 (0.3H, m, H3'' β -p), 4.12–4.09 (0.1H, m, H4'' α -f), 4.06 (1H, dd, $J = 9, 4$ Hz, H4'), 4.05–4.01 (0.6H, m, H3'' α -p), 3.99–3.96 (0.1H, m, H4'' β -f), 3.94 (0.6H, dd, $J = 12.5, 3$ Hz, H5a'' α -p), 3.87 (0.6H, br s, H4'' α -p), 3.85–3.82 (0.3H, m, H4'' β -p), 3.82–3.76 (2H, m, H5'), 3.76–3.73 (0.6H, m, H5'' β -p), 3.70 (0.6H, d, $J = 12.5$ Hz, H5b'' α -p), 3.63–3.59 (0.1H, m, H5b'' α -f), 2.93 (0.3H, ddd, $J = 13.9, 6.9, 6.9$ Hz, H2a'), 2.85 (0.7H, ddd, $J = 13.8, 6.8, 6.8$ Hz, H2a'), 2.57–2.53 (0.1H, m, H2a'' α -f), 2.53–2.46 (1H, m, H2b'),

2.32 (0.1H, ddd, $J = 13.8, 6, 2.3$ Hz, H2a'' β -f), 2.22–2.19 (0.1H, m, H2b'' β -f), 2.16 (0.3H, ddd, $J = 14, 6.3, 2.8$ Hz, H2a'' β -p), 2.09–2.02 (0.6H, m, H2a'' α -p), 2.02–1.99 (0.1H, m, H2b'' α -f), 1.98–1.93 (0.3H, m, H2b'' β -p), 1.93–1.88 (0.6H, m, H2b'' α -p); ¹³C NMR (126 MHz, D₂O) δ 159.2 (C6), 151.8, 151.7 (C2), 151.3 (C4), 139.4, 139.2 (C8), 117.9 (C5), 87.6, 87.5, 87.4 (C4'), 86.5 (C4'' α -f), 86.3 (C4'' β -f), 84.8, 84.7, 84.6, 84.4 (C1'), 82.9 (C1'' β -f), 82.8 (C1'' α -f), 78.7 (C1'' α -p), 76.5 (C1'' β -p), 72.2 (C3'' α -f), 72.1 (C3'' β -f), 71.8, 71.8, 71.5, 71.5 (C3'), 68.2 (C3'' α -p), 67.2 (C4'' β -p), 67.2 (C5'' α -p), 67.1 (C4'' α -p), 66.4 (C3'' β -p), 64.2 (C5'' β -p), 62.6 (C5'' β -f), 62.4 (C5'), 62.3 (C5'' α -f), 62.1 (C5'), 39.5 (C2'' α -f), 39.4 (C2'' β -f), 38.9, 38.8, 38.7 (C2'), 34.9 (C5'' β -p), 33.3 (C5'' α -p).

Analysis of Stability of **9b in Aqueous Buffer.** Compound **9b** (0.4 mg, 1 mM final) was dissolved in 4-(2-hydroxyethyl)-1-piperazineethanesulfonic acid (HEPES) buffer (1 mL, 50 mM, pH 7)

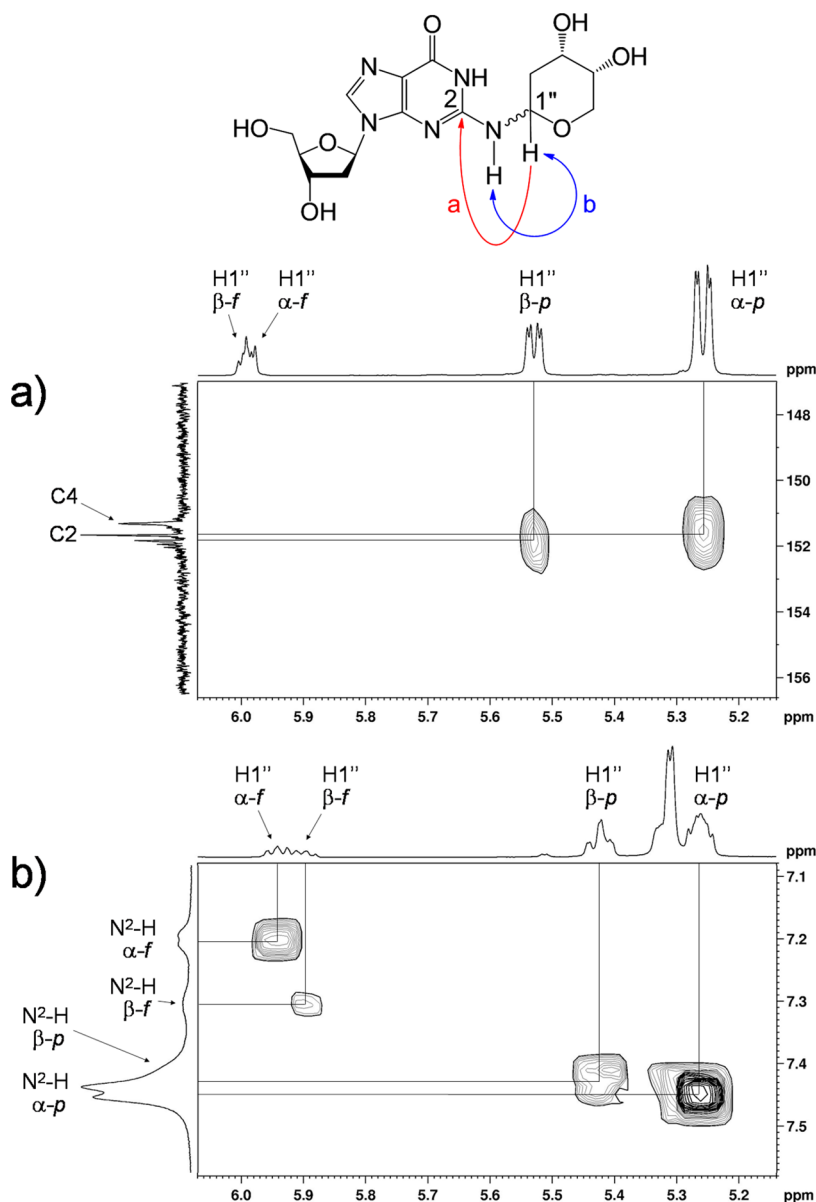


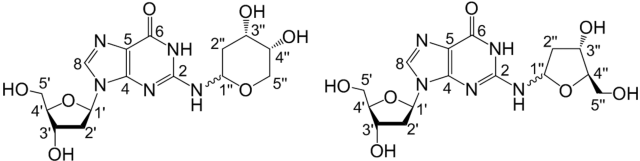
Figure 3. Selected regions of 1H - ^{13}C HMBC and 1H - 1H COSY spectra of **9b** obtained at 500 (1H) and 126 (^{13}C) MHz, respectively. Correlations between (a) $H1''$ and $C2$ in D_2O as well as (b) $H1''$ and N^2-H in $DMSO-d_6$ indicate that the 2-deoxyribose moiety remained attached to N^2 of dG following deprotection.

containing 100 mM NaCl. Decomposition of **9b** to release free dG was monitored by HPLC on an Agilent 1100 series HPLC equipped with autosampler. The reaction was monitored over the course of 34 days at 23 °C, during which time 20 μL aliquots were injected on a Varian Microsorb-MV 100-5 250 \times 4.6 mm C18 column that was eluted with 100% H_2O from 0 to 5 min, 0–10% acetonitrile in H_2O from 5 to 60 min, and 10–0% acetonitrile from 60 to 65 min. Products were monitored by their absorbance at 254 nm. Peak areas were corrected for the relative molar absorptivities of **9b** and dG at 254 nm, which were found to be 13 090 and 12 905 $M^{-1}\cdot cm^{-1}$, respectively. To obtain the apparent first-order rate constant, data for the disappearance of **9b** and the appearance of dG were fit to the appropriate equations for a first-order process.⁴⁵

Gel Electrophoretic Analysis of Stability of 9a and 11a in Duplex DNA. Cross-links were generated as previously described.²¹ Single-stranded 2'-deoxyoligonucleotides were 5'- ^{32}P -labeled by standard procedures. Labeled DNA was annealed with its complementary strand and treated with the enzyme UDG (50 units/mL, final concentration) to generate AP sites. The enzyme was removed by phenol–chloroform extraction. The AP-containing double-stranded

DNA was ethanol-precipitated, resuspended in HEPES buffer (50 mM, pH 7) containing NaCl (100 mM), and incubated at 37 °C for 72 h to generate the dG–AP interstrand cross-link. The reaction mixture was ethanol-precipitated, resuspended in formamide loading buffer, and loaded onto a 20% denaturing polyacrylamide gel. The gel was electrophoresed for 8 h at 200 V to separate cross-linked from uncross-linked DNA. The slower-migrating cross-link band was located by autoradiography and excised from the gel, the gel slice was crushed, and the DNA in the gel was eluted into HEPES buffer (50 mM, pH 7) containing NaCl (100 mM) and incubated at either 37 or 23 °C. Stability of the dG–AP cross-link in duplex DNA was examined by removing aliquots from the assay mixtures at specified time points and freezing them at -20 °C until all the aliquots were collected. The samples were then dissolved in formamide loading buffer and loaded onto a 20% denaturing polyacrylamide gel, and the gel was electrophoresed for 4 h at 1000 V. The amount of radiolabeled DNA in each band on the gel was quantitatively measured by phosphorimager analysis.

Enzymatic Digestion and Mass Spectrometric Analysis. Cross-linked duplex **A** was prepared as described previously.²¹

Table 2. Chemical Shifts and 2D Correlations for 9b in D₂O


position / isomer	δ_c	H _{a/b}	δ_H (J in Hz)	COSY	TOCSY	HMBC ^a	NOESY
2	152.0, 151.9, 151.8, 151.7 ^b						
4	151.3						
5	117.9						
6	159.2					4, 5, 6, 1'	1', 2a', 3', 5'
8	139.4, 139.2	7.94, br s					
1'	84.8, 84.7, 84.6, 84.4	6.35–6.25, m		2a', 2b'	2a', 2b', 3', 4'	4, 8, 3', 4'	8, 2b', 4'
2'	38.9, 38.8, 38.7	a 2.93, ddd (13.9, 6.9, 6.9); 2.85, ddd (13.8, 6.8, 6.8)		1', 2b', 3'	1', 2b', 3', 4', 5'	1', 3', 4'	8, 2b', 3'
		b 2.53–2.46, m		1', 2a', 3'	1', 2a', 3', 4', 5'	3', 4'	1', 2a', 3', 4'
3'	71.8, 71.7, 71.5, 71.5	4.67–4.62, m		2a', 2b', 4'	1', 2a', 2b', 4', 5'	1'	8, 2a', 2b', 4', 5'
4'	87.6, 87.5, 87.4	4.06, dd (9, 4)		3', 5'	1', 2a', 2b', 3', 5'	3'	3', 5'
5'	62.1	3.82–3.76, m		4'	2a', 2b', 3', 4'	3'', 4''	8, 3', 4'
1'' α -p	78.7	5.26, dd (9.5, 2.5)		2a'', 2b''	2a'', 2b'', 3'', 4''	2, 3''	2a'', 3'', 5b''
1'' β -p	76.5	5.54, dd (8, 2.5)		2a'', 2b''	2a'', 2b'', 3''	2, 3''	2a'', 5''
1'' α -f	82.8	6.00–5.98, m		2a'', 2b''	2a'', 2b'', 3''	3'', 4''	2a''
1'' β -f	82.9	6.02–6.00, m		2a'', 2b''	2a'', 2b'', 3''	3'', 4''	2a''
2'' α -p	33.3	a 2.09–2.02, m		1'', 2b'', 3''	1'', 2b'', 3'', 4''	1'', 5''	1'', 2b'', 3''
		b 1.93–1.88, m		1'', 2a'', 3''	1'', 2a'', 3'', 4''	1'', 5''	2a''
2'' β -p	34.9	a 2.16, ddd (14, 6.3, 2.8)		1'', 2b'', 3''	1'', 2b'', 3''	5''	1'', 2b'', 3''
		b 1.98–1.93, m		1'', 2a'', 3''	1'', 2a'', 3''		2a'', 3''
2'' α -f	39.5	a 2.57–2.53, m		1'', 2b'', 3''	1'', 2b'', 3''		1'', 2b''
		b 2.02–1.99, m		1'', 2a'', 3''	1'', 2a'', 3''		2a''
2'' β -f	39.4	a 2.32, ddd (13.8, 6, 2.3)		1'', 2b''	1'', 2b'', 3''		1'', 2b''
		b 2.22–2.19, m		1'', 2a'', 3''	1'', 2a'', 3''	1''	2a''
3'' α -p	68.2	4.05–4.01, m		2a'', 2b'', 4''	1'', 2a'', 2b'', 4''		1'', 2a'', 4''
3'' β -p	66.4	4.22–4.18, m		2a'', 2b''	1'', 2a'', 2b'', 5''		2a'', 2b'', 4''
3'' α -f	72.2	4.40–4.37, m		2a'', 2b''	1'', 2a'', 2b'', 4'', 5b''		2a'', 5''
3'' β -f	72.1	4.43–4.40, m		2b''	1'', 2a'', 2b'', 4''		2b''
4'' α -p	67.1	3.87, br s		3''	1', 2a'', 2b'', 3'', 5a'', 5b''	2', 3''	3''
4'' β -p	67.2	3.85–3.82, m			3'', 5''		3''
4'' α -f	86.5	4.12–4.09, m		5b''	3'', 5b''	1''	5''
4'' β -f	86.3	3.99–3.96			3''		
5'' α -p	67.2	a 3.94, dd (12.5, 3)		5b''	4'', 5b''	1'', 3''	5b''
		b 3.70, d (12.5)		5a''	4'', 5a''	1''	1'', 5a''
5'' β -p	64.2	3.76–3.73, m			3''	1''	1''
5'' α -f	62.3	b 3.63–3.59, m		4''	4''		3''
5'' β -f	62.6						

^aHMBC correlations are from protons in the δ_H column to the listed carbon(s). ^bMultiple ¹³C peaks arise from the four isomers of 9b.

To 500 pmol of the duplex DNA sample was added a cocktail of enzymes including nuclease P1 (1 unit), phosphodiesterase I (0.005 unit), phosphodiesterase II (0.005 unit), and alkaline phosphatase (1 unit), as described previously.⁴⁶ To inhibit contaminating adenosine deaminase activity during digestion, erythro-9-(2-hydroxy-3-nonyl)adenine was also added to the digestion mixture at a final concentration of 2.5 mM. Enzymes in the digestion mixture were removed by chloroform extraction, the aqueous layer was dried in a Speed-vac, and the residue was reconstituted in water and subjected to mass spectrometric analyses.

The LC-MS/MS and -MS/MS/MS experiments were conducted on an LTQ linear ion trap mass spectrometer (Thermo Fisher Scientific). Samples were loaded and separated on a 0.5 × 250 mm Zorbax SB-C18 column (5 μ m beads, 80 Å pore size; Agilent Technologies,

Santa Clara, CA) at a flow rate of 8.0 μ L/min. A solution of 0.1% (v/v) formic acid in water (A) and a solution of 0.1% (v/v) formic acid in methanol (B) were used as mobile phases, and the gradient included 5 min, 0–20% B; 35 min, 20–50% B 10 min, 50% B; and 1 min, 50–0% B.

RESULTS AND DISCUSSION

Synthesis and Spectroscopic Characterizations of Unreduced Cross-Link Remnant 9b. Our initial attempts to prepare 9b involved simply mixing 2-deoxyribose (dR) with 2'-deoxyguanosine (dG). This approach held some promise because, in a number of other cases, the reaction of an aldehyde-containing molecule with unprotected dG yields the

Table 3. Chemical Shifts and 2D Correlations for 11b in D₂O

position	δ_C	H _{a/b}	δ_H (J in Hz)	COSY	TOCSY	HMBC ^a	NOESY
2	153.3						
4	152.1						
5	116.6						
6	159.6						
8	138.4		7.88, s			4, 5, 6, 1'	1', 2a', 3', 5a', 5b'
1'	84.5		6.25, t (6.8)	2a', 2b'	2a', 2b', 3', 4'	4, 8, 2', 3', 4'	8, 2a', 2b', 4'
2'	38.7	a	2.86, ddd (13.9, 6.9, 6.9)	1', 2b', 3'	1', 2b', 3', 4'	1', 3', 4'	1', 2b', 3'
		b	2.47, ddd (14.0, 6.5, 4)	1', 2a', 3'	1', 2a', 3', 4'	3', 4'	1', 2a', 3', 4'
3'	71.7		4.61, dt (6.5, 4)	2a', 2b', 4'	1', 2a', 2b', 4', 5a', 5b'	1', 5'	8, 2a', 2b', 5a', 5b'
4'	87.4		4.06, dt (5.5, 4)	3', 5a', 5b'	1', 2a', 2b', 3', 5a', 5b'	1', 3'	1', 2b'
5'	62.2	a	3.79, dd (12.5, 4)	5b'	3', 4', 5b'	3', 4'	8, 3'
		b	3.74, dd (12.5, 6.5)	5a'	3', 4', 5a'	3', 4'	8, 3'
1''	38.5		3.49–3.44, m	2a'', 2b''	2a'', 2b'', 3'', 4''	2, 2'', 3''	2a'', 2b'', 3''
2''	32.0	a	2.00–1.91, m	1'', 2b'', 3	1'', 2b'', 3'', 4''	1'', 3'', 4''	1'', 2b'', 3'', 5b''
		b	1.71–1.61, m	1'', 2a'', 3''	1'', 2a'', 3'', 4''	1'', 3'', 4''	1'', 2a'', 3'', 5a''
3''	70.1		3.71–3.67, m	2a'', 2b''	1'', 2a'', 2b'', 4'', 5a'', 5b''	1'', 2'', 4''	1'', 4''
4''	75.2		3.64–3.61, m		1'', 2a'', 2b'', 3'', 5a'', 5b''	2''	3''
5''	63.1	a	3.73, dd (18.8, 8.8)	5a''	3'', 4'', 5b''		2b''
		b	3.59, dd (19.3, 6.8)	5b''	3'', 4'', 5a''	3'', 4''	2a''

^aHMBC correlations are from protons in the δ_H column to the listed carbon(s).

corresponding *N*²-adduct.^{4,6,14,47,48} Accordingly, we examined the reaction of dG (40 mM) with dR (120 mM) in sodium acetate buffer (200 mM, pH 4) or a mixture of methanol/water/acetic acid (8:1:4).⁴⁹ Unfortunately, no detectable amounts of product were observed under these conditions as judged by thin-layer chromatographic analysis.

We undertook an alternative approach to the synthesis of **9b** involving reaction of an activated 2-deoxyribose donor with a protected dG derivative. Our approach was based on the route used by Takamura-Enya et al.⁵⁰ for the synthesis of *N*²-(*D*-ribose-1-yl)-2'-deoxyguanosine. We prepared the protected 2'-deoxyguanosine analogue **12** by reaction of dG with *t*-butyldimethylsilyl chloride,⁴² followed by a Mitsunobu reaction with 2-(trimethylsilyl)ethanol to install the (2-trimethylsilyl)ethyl group at O⁶ of the guanine residue (Scheme 4).⁵¹ The 2-deoxyribose donor, 3,5-bis(*t*-butyldimethylsilyl)-2-deoxyribose-1-iodide was generated in situ via reaction of 1,3,5-tris(*t*-butyldimethylsilyl)-2-deoxyribose **13** with trimethylsilyl iodide (TMS-I) in CH₂Cl₂ at -78 °C, and to this mixture was added a solution of **12** and diisopropylethylamine (DIEA) in CH₂Cl₂ (Scheme 5). Our use of a 2-deoxyribose iodide rather than the previously reported ribosyl iodide necessitated some modifications of the literature method,⁵⁰ including lower reaction temperatures, a larger excess of the iodide, and greater equivalents of DIEA. The reaction generated a major product **14** that eluted faster than **12** on silica gel and was isolated in 54% yield by column chromatography.

Product **14** was fully characterized by NMR spectroscopy. One-dimensional (1D) ¹H NMR and ¹H–¹H COSY spectra revealed resonances associated with the dG nucleoside⁵² alongside resonances from the 3,5-bis(*t*-butyldimethylsilyl)-2-deoxyribose unit. The ¹³C resonances associated with each carbon were assigned by use of heteronuclear multiple-quantum

correlation (HMQC) and heteronuclear multiple-bond correlation (HMBC) spectra. Two-dimensional (2D) NMR spectra further provided evidence that the 3,5-(*tert*-butyldimethylsilyl)-2-deoxyribose adduct was attached to the exocyclic *N*²-position of the guanine residue as expected. Specifically, the ¹H–¹H correlation spectroscopy (COSY) experiment showed a correlation between *N*²-H of the guanine residue and H1'' of the 3,5-bis(*tert*-butyldimethylsilyl)-2-deoxyribose adduct (Figure 1). In addition, the HMBC experiment showed correlations between C2 of the guanine residue and H1'', along with a correlation between *N*²-H and C2''.

A doubling of resonances associated with the 3,5-bis(*tert*-butyldimethylsilyl)-2-deoxyribose adduct in **14** indicated that this moiety was present as a mixture of isomers. Careful inspection of the NMR spectra suggested that the mixture consisted of a 4:1 diastereomeric mixture of α - and β -anomers of the furanose form of the sugar (Scheme 5). This assessment was based upon the chemical shifts of C4'' in the two isomers of **14** at 86.7 and 87.0 parts per million (ppm), values consistent with a furanose sugar.⁵³ The major isomer showed a strong nuclear Overhauser effect (NOE) cross-peak between guanine *N*²-H and H4'', consistent with the α -isomer, while the minor isomer showed a stronger NOE cross-peak between H1'' and H4'', consistent with the β -isomer (Figure 2).⁴⁴ The high-resolution mass spectrum was consistent with the molecular formula expected for **14**.

Overall, the spectral data provided evidence that coupling of **12** with 2-deoxyribose iodide generated the desired product **14**. While this product has the potential to exist as either a ring-opened imine or a cyclic hydroxyalkylhemiaminal, the C1'' chemical shift at 83.6 ppm for this product was consistent with the cyclic structure of **14**.⁵³ The corresponding imine ¹³C-chemical shift would be expected at approximately 160 ppm.²⁰

The observed HMBC correlation between H1'' and C4'' also was consistent with the ring-closed isomer of **14**. Table 1 provides a complete list of the chemical shifts and 2D NMR correlations for **14**.

The silyl protecting groups were removed from **14** by treatment with tetrabutylammonium fluoride (TBAF) in THF to generate a new product in 59% yield. As expected, the NMR spectrum of the deprotected material **9b** was more complex than that of the starting material **14** because removal of the protecting groups from the 2-deoxyribose adduct enables interconversion between pyranose and furanose forms, each of which can exist as a mixture of α - and β -isomers (Scheme 5).^{53–56} Two-dimensional NMR experiments provided evidence that the 2-deoxyribose adduct in **9b** remained connected at the exocyclic N²-amino group of the guanine residue. As described above in the context of **14**, the ¹H–¹H COSY spectrum of **9b** in DMSO-*d*₆ showed a correlation between N²-H and H1'' of the 2-deoxyribose adduct (Figure 3). Again, the HMBC spectrum showed a correlation between C2 of the guanine residue and H1''. Observation of the N1-imino proton at 10.9 ppm in the ¹H NMR spectrum in DMSO-*d*₆ further provided evidence against attachment of the adduct at N1. Overall, the NMR spectral data provided evidence that the 2-deoxyribose adduct remained attached at the exocyclic N²-amino group of the guanine residue as shown in **9b**.

All four of the anticipated isomers arising from equilibration of the 2-deoxyribose adduct were observed in the NMR spectra of **9b**. Similar to **14**, the positions of the ¹³C shifts of C4'' in the isomers of **9b**, along with the results of NOE experiments, allowed us to assign key resonances to each of the four isomers and determine that the 2-deoxyribose adduct connected to N² of the guanine residue exists as a 6:2:1:1 mixture of α -pyranose, β -pyranose, α -furanose, and β -furanose isomers. This is consistent with the observation that pyranose isomers of unprotected 2-deoxyribose and its arylamino-2-deoxyriboside analogues typically predominate in solution.^{53–56} The chemical shifts of C1'' in the isomers of **9b** at 76.5–82.9 ppm, along with HMBC correlations observed between H1'' and C4'' in the furanose isomers and between H5'' and C1'' in the pyranose isomers, were again consistent with the cyclic hydroxyalkylhemiaminal form. No evidence for a ring-opened imine isomer was seen in the NMR spectra. Predominance of the cyclic isomer is consistent with literature reports for structurally related compounds.^{14,48,57} The ¹H NMR chemical shifts of key positions such as H1'', N²-H, H8, and N1-H in **9b** were similar to those observed for related DNA adducts.^{14,48,57} Table 2 provides a complete list of the chemical shifts and 2D NMR correlations for **9b**. High-resolution mass spectrometric analysis was consistent with the molecular formula expected for **9b**. When the compound was dissolved in D₂O and subjected to ESI-MS analysis with the use of an equivolume mixture of D₂O and acetonitrile as the spray solvent, a mass increase of 6 amu was observed, consistent with the presence of six exchangeable hydrogens in **9b** (Figure S25, Supporting Information).

Synthesis and Spectroscopic Characterization of Reduced Cross-Link Remnant 11b. In our previous characterization of the dG–AP cross-link in duplex DNA, we employed conditions of reductive amination¹⁸ to generate good yields of a chemically stable cross-linked species, whose structure was tentatively assigned as **11a** (Scheme 3).^{21,22} Reduction of imine and cyclic hydroxyalkylhemiaminal adducts attached at the N²-amino group of guanine residues has been used by others to facilitate the detection and analysis of aldehyde-derived DNA

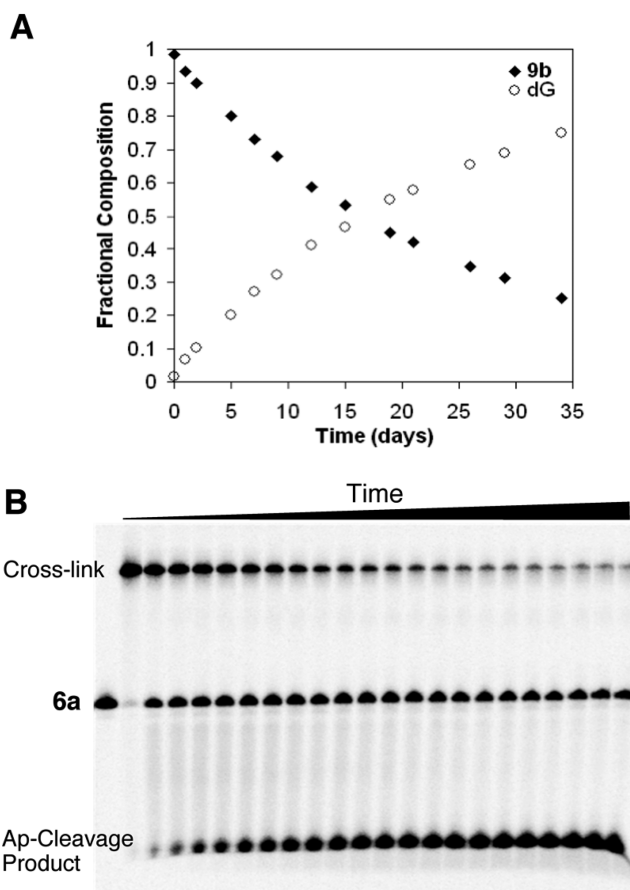


Figure 4. Stability of dG–AP cross-linkage. (A) Synthetic cross-link remnant **9b** was incubated at 23 °C in HEPES buffer (pH 7, 50 mM) containing NaCl (100 mM). Disappearance of **9b** and concomitant appearance of dG were monitored by HPLC. (B) Gel electrophoretic analysis of purified, unreduced cross-link in duplex **A**, incubated at 37 °C in HEPES buffer (50 mM, pH 7) containing NaCl (100 mM). The fast-moving fragment at the bottom of the gel corresponds to the 3'-4-hydroxy-2-penten-5-phosphate cleavage product resulting from β -elimination at the AP site.

adducts.^{4,14,19,20,48} To elucidate the structure of the reduced dG–AP cross-link in DNA, we wished to prepare a synthetic standard for the proposed structure of the reduced dG–AP cross-link remnant **11b**. Toward this end, we treated the protected dG–dR derivative **14** with NaCNBH₃ in methanol–acetic acid. The silyl groups were then removed from the crude product by treatment with TBAF in THF, and the resulting material was purified by column chromatography on silica gel eluted with 15:5:1 CH₂Cl₂/CH₃OH/H₂O. As anticipated, the NMR spectra of the product **11b** were greatly simplified compared to those of either **14** or **9b**, consistent with loss of the potential for pyranose–furanose and anomeric isomerism (Scheme 5). Significant changes were especially evident at the C1'' position of the reduced adduct. The splitting patterns and integrations associated with the H1'' and H2'' protons were diagnostic for the presence of a CH₂ group at C1''. The resonances for the H1'' protons appeared at 3.44–3.49 ppm, a range consistent with the published data for an analogous structure.⁵⁸ The ¹³C shift of C1'' changed dramatically from 76.5 to 82.9 ppm in **9b** to 38.5 ppm in **11b**, consistent with the acyclic alkyl adduct in **11b**. As described above in the context of **14** and **9b**, ¹H–¹H COSY and HMBC spectra of **11b** provided evidence for attachment of the 2-deoxyribose unit at the

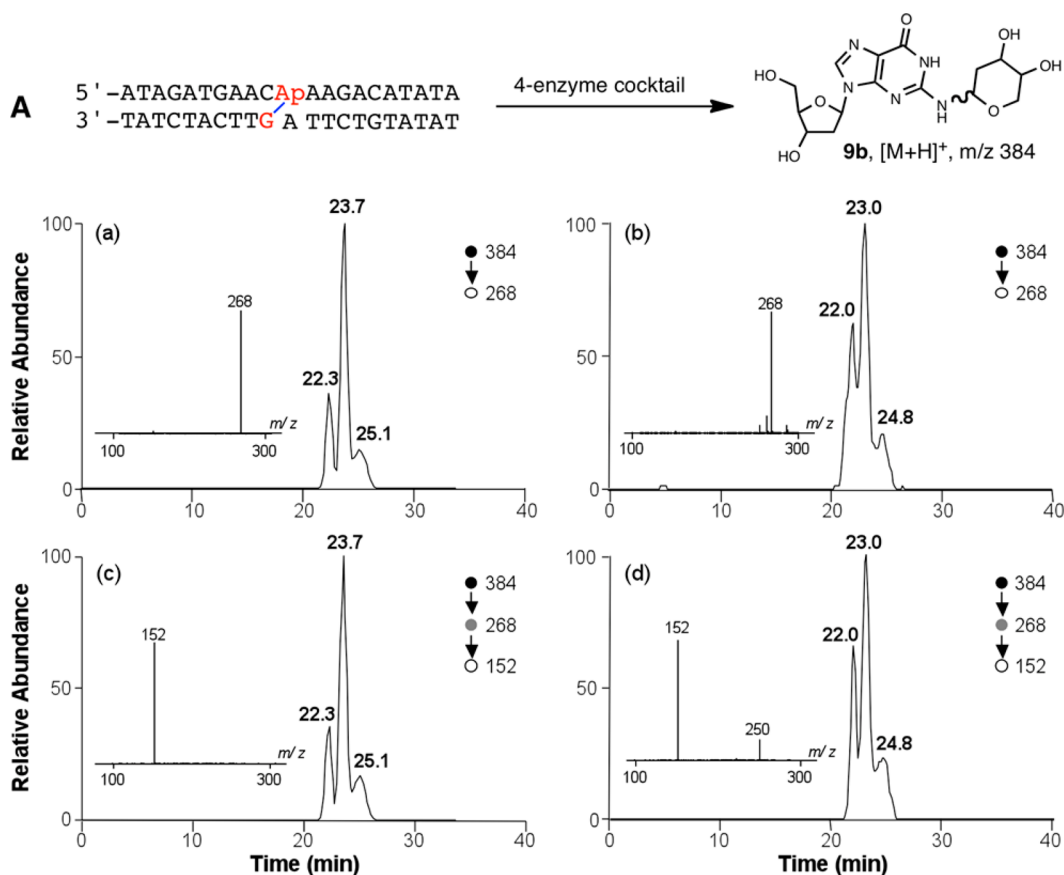


Figure 5. LC-MS/MS and MS/MS/MS for characterization of the dG-AP cross-link remnant that was obtained synthetically (a and c) or released from purified AP-derived cross-link-containing duplex DNA sequence A (b and d). (a, b) Selected-ion chromatograms for monitoring the loss of 2-deoxyribose (i.e., m/z 384 \rightarrow 268 transition) from [M + H]⁺ ion of the unreduced dG-AP cross-link remnant that was (a) obtained synthetically or (b) liberated from the four-enzyme digestion of purified cross-link-containing duplex DNA. (c, d) Corresponding selected-ion chromatograms for monitoring the formation of [M + H]⁺ ion of guanine (i.e., m/z 384 \rightarrow 268 \rightarrow 152 transition) from the ion of m/z 268 observed in MS/MS. Depicted in the insets are the corresponding MS/MS and MS/MS/MS averaged from the retention times of (a, c) 23.7 min and (b, d) 23.0 min. The MS/MS/MS averaged from the two other peaks are displayed in Figure S26. The ion of m/z 250 in panel d is attributed to isobaric interference.

N^2 -position of the guanine residue. Observation of the N1-imino proton at 10.6 ppm in the ¹H NMR spectrum in DMSO-*d*₆ provided evidence against attachment of the adduct at N1. The ¹³C chemical shifts of the guanine residue in **14** were similar (± 3.5 ppm or less) to those in the native nucleoside dG and in other known N^2 -alkyl-dG adducts.^{59,60} Table 3 provides a complete list of the chemical shifts and 2D-NMR correlations for **11b**. Plots of NMR and UV-vis spectra for **14**, **9b**, and **11b** are provided in Supporting Information. In addition, ESI-MS analysis of **11b** in H₂O and D₂O revealed the presence of seven exchangeable protons in the [M + Na]⁺ ion of the compound, which is consistent with the proposed structure (Figure S25, Supporting Information).

Stability of Unreduced Cross-Link Remnant 9b and Native Interstrand DNA-DNA Cross-Link. The formation of N -aryl aminoglycosides is reversible.^{61,62} Consequently, we recognized that the cross-link remnant **9b** had the potential to revert to dG and 2-deoxyribose. Therefore, before employing **9b** as an analytical standard, we examined the stability of this material. We used HPLC to monitor the stability of **9b** (1 mM) at 23 °C in HEPES buffer (50 mM, pH 7) containing NaCl (100 mM). Our results indicated that **9b** was quite stable under these conditions, disappearing with a half-life of approximately 17 days (corresponding to a first-order rate constant of

4×10^{-2} day⁻¹). As expected, decomposition of **9b** was accompanied by release of the native nucleoside dG (Figure 4). The stability of **9b** was also monitored by thin-layer chromatography (Figure S19, Supporting Information).

We compared the stability of cross-link remnant **9b** to that of the dG-AP cross-link in duplex DNA. Accordingly, we generated the dG-AP cross-link in a ³²P-labeled version of the 21 base pair duplex A (5'-³²P-labeled on the top strand) and isolated the cross-linked DNA by gel electrophoresis. Dissociation of the cross-linked DNA into the single strand **6a** in HEPES buffer (50 mM, pH 7) containing NaCl (100 mM) at 23 °C was monitored by gel electrophoresis. The cross-linked DNA decomposed with apparent first-order kinetics and a half-life of approximately 22 days ($k = 3.1 \times 10^{-2}$ day⁻¹; Figure 4B and Figure S20 in Supporting Information). Overall, the stability of dG-AP cross-link in duplex DNA mirrors that of cross-link remnant **9b**.

At pH 5.6 and 37 °C, cross-link remnant **9b** decomposed with a half-life of 7.7 days (30 mM sodium acetate, pH 5.6, containing 1 mM ZnCl₂; Figure S17, Supporting Information). These solvent conditions resemble those employed during enzymatic digestion of DNA prior to mass spectrometric analysis.

Evidence for Release of Cross-Link Remnants 9b and 11b from DNA Duplexes Containing Native and Reduced dG-AP Cross-Link. With a synthetic standard of

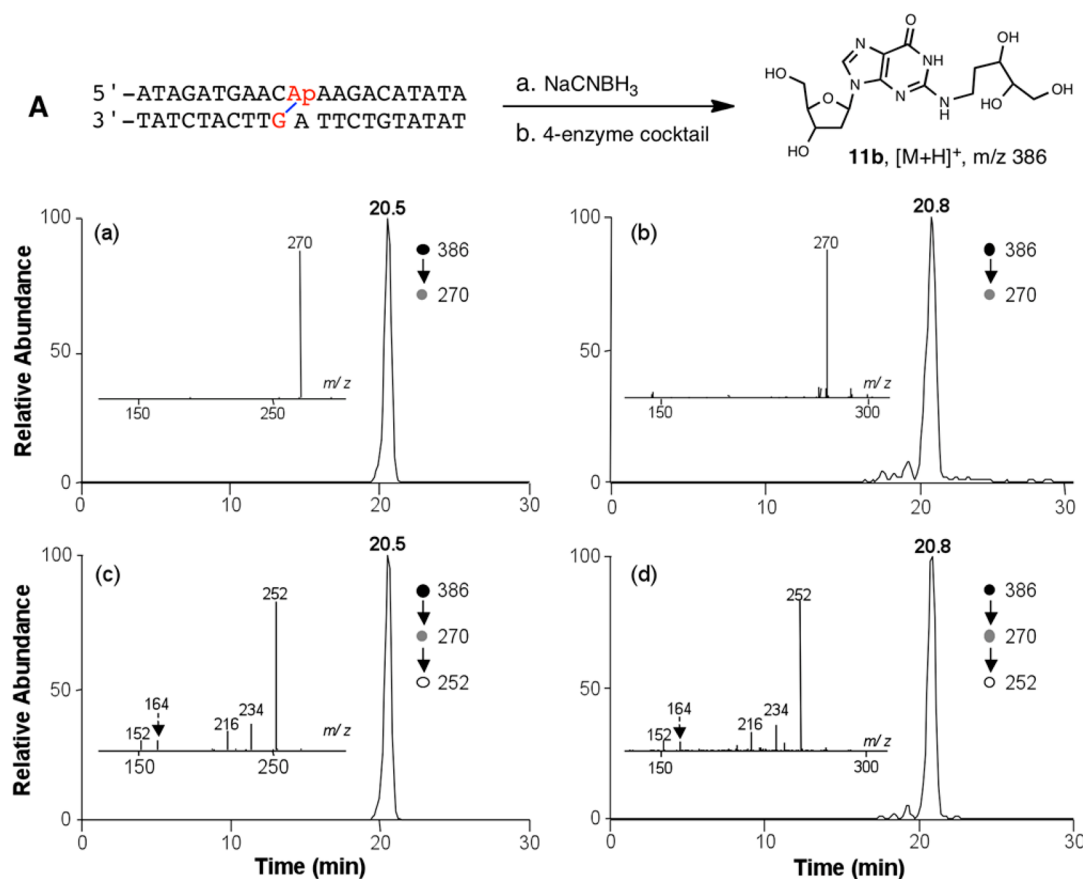


Figure 6. LC-MS/MS and MS/MS/MS for characterization of reduced dG–AP cross-link remnant that was obtained synthetically or released from NaCNBH₃-treated cross-linked duplex DNA. Shown are selected-ion chromatograms for monitoring the loss of a 2-deoxyribose (i.e., m/z 386 \rightarrow 270 transition) from the [M + H]⁺ ion of reduced dG–AP cross-link remnant that was (a) obtained synthetically or (b) released from the 4-enzyme digestion of reduced product of the purified cross-linked duplex **A**. (c, d) Corresponding selected-ion chromatograms for monitoring the further loss of H₂O from the ion at m/z 270 observed in MS/MS (i.e., m/z 386 \rightarrow 270 \rightarrow 252 transition). (Insets) Corresponding MS/MS and MS/MS/MS averaged from retention times of (a, c) 20.5 and (b, d) 20.8 min.

the cross-link remnant **9b** in hand, we set out to determine whether this was, in fact, the structure of the authentic cross-link remnant released by enzymatic digestion of a DNA duplex containing the dG–AP cross-link. Duplex **A**, containing the dG–AP cross-link, was prepared as previously described.²¹ Briefly, an abasic site was site-selectively introduced into the duplex by treatment of the corresponding 2'-deoxyuridine-containing duplex with uracil-DNA glycosylase (UDG). The AP-derived cross-link was generated in duplex DNA by incubation in HEPES buffer (50 mM, pH 7) containing NaCl (100 mM) at 37 °C. The dG–AP cross-link was generated in approximately 2–3% yield in this sequence under these conditions.²¹ The resulting native (unreduced) cross-link was digested with a four-enzyme cocktail that included nuclease P1, alkaline phosphatase, and phosphodiesterases I and II. This treatment led to the liberation of the fully digested dG–AP cross-link (Figure 5). The digestion mixture was subjected to LC-MS/MS and MS/MS/MS analysis on an LTQ linear ion trap mass spectrometer, under previously reported experimental conditions.^{63–65} We also analyzed the synthetic dG–AP cross-link remnant (**9b**) by LC-MS/MS and MS/MS/MS under the same experimental conditions.

The LC-MS/MS results revealed that collisional activation of the [M + H]⁺ ions of **9b** led to formation of a dominant fragment ion of m/z 268. The selected-ion chromatogram (SIC) for the m/z 384 \rightarrow 268 transition showed three major

peaks at 22.3, 23.7, and 25.1 min. The presence of multiple peaks in the SIC is in agreement with the fact that **9b** exists as an isomeric mixture of α - and β -anomers of both pyranose and furanose forms (vide supra). Further collisional activation of the ion of m/z 268 resulted in facile formation of the protonated ion of guanine at m/z 152. Similar LC-MS/MS analysis of the aforementioned enzymatic digestion mixture of purified cross-link-containing duplex **A** also revealed three major peaks at 22.0, 23.0, and 24.8 min in the SIC for the m/z 384 \rightarrow 268 transition (Figure 5b). Further collisional activation of the ion at m/z 268 again gave rise to formation of the ion at m/z 152 as the major fragment ion in MS/MS/MS (Figure 5 and Figure S26 in Supporting Information). The similar HPLC elution time, as well as the similar fragmentation behaviors observed in MS/MS and MS/MS/MS, suggested strongly that the cross-link remnant released from duplex DNA shares the same structure as synthetic cross-link **9b**.

We next generated the reduced dG–AP cross-link in duplex **A** by incubation of the AP-containing duplexes in sodium acetate buffer (750 mM, pH 5.2) containing NaCNBH₃ (250 mM) at 37 °C for 24 h, as previously described.²¹ Digestion of the duplex containing the reduced cross-link, followed by LC-MS/MS analysis, revealed a major peak eluting at 20.8 min in the SIC for the m/z 386 \rightarrow 270 transition (Figure 6). The synthetic reduced cross-link remnant **11b** displayed very similar retention time and nearly identical

fragmentation patterns in MS/MS and MS/MS/MS as that released from duplex DNA (Figure 6). In this regard, the sequential losses of multiple H₂O molecules in MS/MS/MS of the reduced dG-AP remnant, which differ from the predominant loss of the 2-deoxyribose remnant observed for the corresponding MS/MS/MS of the unreduced dG-AP remnant, are also consistent with the ring-opened structure of the reduced derivative. Together, these results provided further evidence regarding the structural nature of the dG-AP cross-link in duplex DNA.

CONCLUSIONS

The goals of this work were to characterize the chemical structure and properties of dG-AP cross-links generated in duplex DNA. Our approach centered upon characterization of the nucleoside cross-link “remnant” released by enzymatic digestion of a DNA duplex containing the dG-AP cross-link.²¹ Accordingly, our work began with the chemical synthesis of an analytical standard of the putative cross-link remnant **9b**, composed of a 2-deoxyribose adduct attached to the exocyclic N²-amino group of dG. NMR spectroscopic analysis revealed that the 2-deoxyribose adduct in **9b** exists as an equilibrating mixture of the ring-closed α -pyranose, β -pyranose, α -furanose, and β -furanose isomers (Scheme 5). A synthetic standard for the reduced cross-link remnant **11b** was prepared by treatment of **14** with NaCNBH₃, followed by removal of protecting groups. Reduction ablates the stereocenter at C1'' of the 2-deoxyribose adduct to give **11b** as a single entity lacking the isomeric complexity of the unreduced remnant **9b**.

LC-MS/MS analysis revealed that the retention times and mass spectral properties of the synthetic cross-link remnants **9b** and **11b** matched materials generated by enzymatic digestion of DNA duplexes containing native and reduced dG-AP cross-link, respectively. This provided evidence that the dG-AP cross-link formed at 5'-CAP/AG sequences in duplex DNA²¹ involves attachment of the exocyclic N²-amino group of dG to the aldehydic carbon of the AP-site on the opposing strand of the duplex. The LC-MS/MS methodology reported here provides a foundation for detection of the dG-AP cross-links **9b** and **11b** in cellular DNA. Analogous to some other aldehyde-derived DNA adducts,^{20,66} the native (unreduced) dG-AP cross-link in duplex DNA has the potential to exist in several different forms (Scheme 3), and the exact distribution of these cross-link isomers present in duplex DNA remains to be determined.

We also examined the chemical stability of cross-links **9** and **11** in both the synthetic nucleoside remnants and duplex DNA. As expected, the reduced cross-link **11** was completely stable in the remnant and in duplex DNA (Figure S24). More interestingly, we found that the unreduced cross-link remnant **9b** was quite stable in aqueous buffered solution, decomposing with a half-life of 17 days at pH 7 and 23 °C. Cyclization of the C4''-OH group onto the imine residue in **8** may serve to limit the amount of hydrolytically labile imine present in solution, thus stabilizing the cross-link.^{67–69} Consistent with this notion, it is known that N-aryl aminoglycosides that exist as cyclic hydroxyalkylhemiaminals typically undergo hydrolysis with half-lives in the range of hours to days at pH values near neutral.^{70–72} In contrast, simple imines that lack this protective “hydroxyl lock” mechanism are hydrolytically labile. For example, the half-life for hydrolysis of N-p-chlorobenzylideneaniline in aqueous buffer at pH 7 and 25 °C is approximately 3.5 min (see Figure 4 in ref 73). Most interestingly, the stability of the cross-link attachment observed in the nucleoside remnant was reflected in the properties of the cross-link in duplex DNA. We found

that the cross-link in duplex DNA decomposed with a half-life of 22 days at pH 7 and 23 °C. The intrinsic chemical stability of the dG-AP linkage in duplex DNA suggests that this cross-link may have the power to block cellular DNA-processing enzymes involved in transcription and replication.

ASSOCIATED CONTENT

Supporting Information

Twenty-seven figures, showing 1D and 2D NMR spectra of **9b**, **11b**, **12**, **13**, and **14**; UV absorption spectra; HPLC and TLC chemical kinetics analysis of stability of **9b** and **11b**; gel electrophoretic analysis of stability of cross-links **9a** and **11a** in duplex DNA; ESI-MS of **9b** and **11b**; and MS/MS/MS analysis of **9b** released by enzymatic digestion of cross-linked duplex A. This material is available free of charge via the Internet at <http://pubs.acs.org/>.

AUTHOR INFORMATION

Corresponding Author

*gatesk@missouri.edu

Notes

The authors declare no competing financial interest.

ACKNOWLEDGMENTS

We are grateful to the National Institutes of Health for support of this work (ES021007).

REFERENCES

- (1) Gates, K. S. In *Comprehensive Natural Products Chemistry*; Kool, E. T., Ed.; Pergamon: New York, 1999; Vol. 7, pp 491–552.
- (2) Delaney, J. C.; Essigmann, J. M. *Chem. Res. Toxicol.* **2008**, *21*, 232–252.
- (3) Marnett, L. J. In *DNA Adducts: Identification and Biological Significance*; Hemminki, K., Dipple, A., Shuker, D. E. G., Kadlubar, F. F., Segerback, D., Bartsch, H., Eds.; IARC Scientific Publications: Lyon, France, 1994; Vol. 125, pp 151–162.
- (4) Wang, M.; McIntee, E. J.; Cheng, G.; Shi, Y.; Villalta, P. W.; Hecht, S. S. *Chem. Res. Toxicol.* **2000**, *13*, 1149–1157.
- (5) Shapiro, R.; Cohen, B. I.; Shiuiey, S.-J.; Maurer, H. *Biochemistry* **1969**, *8*, 238–245.
- (6) Chaw, Y. F. M.; Crane, L. E.; Lange, P.; Shapiro, R. *Biochemistry* **1980**, *19*, 5525–5531.
- (7) Wang, H.; Marnett, L. J.; Harris, T. M.; Rizzo, C. J. *Chem. Res. Toxicol.* **2004**, *17*, 144–149.
- (8) Olsen, R.; Molander, P.; Øvrebo, S.; Ellingsen, D. G.; Thorud, S.; Thomassen, Y.; Lundanes, E.; Greibrokk, T.; Backman, J.; Sjöholm, R.; Kronberg, L. *Chem. Res. Toxicol.* **2005**, *18*, 730–739.
- (9) Wang, M.; McIntee, E. J.; Cheng, G.; Shi, Y.; Villalta, P. W.; Hecht, S. S. *Chem. Res. Toxicol.* **2000**, *13*, 1065–1074.
- (10) Lee, W. H.; Rindgen, D.; Bible, R. H. J.; Hajdu, E.; Blair, I. A. *Chem. Res. Toxicol.* **2000**, *13*, 565–574.
- (11) Garcia, C. C. M.; Angeli, J. P. F.; Freitas, F. P.; Gomes, O. F.; de Oliveira, T. F.; Loureiro, A. P. M.; Di Mascio, P.; Medeiros, M. H. G. *J. Am. Chem. Soc.* **2011**, *133*, 9140–9143.
- (12) McGhee, J. D.; von Hippel, P. H. *Biochemistry* **1975**, *14*, 1281–1296.
- (13) McGhee, J. D.; von Hippel, P. H. *Biochemistry* **1975**, *14*, 1297–1303.
- (14) Young-Sciame, R.; Wang, M.; Chung, F.-L.; Hecht, S. M. *Chem. Res. Toxicol.* **1995**, *8*, 607–616.
- (15) Yuan, B.; Cao, H.; Jiang, Y.; Hong, H.; Wang, Y. *Proc. Natl. Acad. Sci. U.S.A.* **2008**, *105*, 8679–8684.
- (16) Wang, M.; Yu, N.; Chen, L.; Villalta, P. W.; Hochalter, J. B.; Hecht, S. M. *Chem. Res. Toxicol.* **2006**, *19*, 319–324.

- (17) Cho, Y.-J.; Wang, H.; Kozekov, I. D.; Kurtz, A. J.; Jacob, J.; Voehler, M.; Smith, J.; Harris, T. M.; Lloyd, R. S.; Rizzo, C. J.; Stone, M. P. *Chem. Res. Toxicol.* **2006**, *19*, 195–208.
- (18) Borch, R. F.; Hassid, A. I. *J. Org. Chem.* **1972**, *37*, 1673–1674.
- (19) Lu, K.; Moeller, B.; Doyle-Eisele, M.; McDonald, J. P.; Swenberg, J. A. *Chem. Res. Toxicol.* **2011**, *24*, 159–161.
- (20) Cho, Y.-J.; Kim, H.-Y.; Huang, H.; Slutsky, A.; Minko, I. G.; Wang, H.; Nechev, L. V.; Kozekov, I. D.; Kozekova, A.; Tamura, P.; Jacob, J.; Voehler, M.; Harris, T. M.; Lloyd, R. S.; Rizzo, C. J.; Stone, M. P. *J. Am. Chem. Soc.* **2005**, *127*, 17686–17696.
- (21) Johnson, K. M.; Price, N. E.; Wang, J.; Fekry, M. I.; Dutta, S.; Seiner, D. R.; Wang, Y.; Gates, K. S. *J. Am. Chem. Soc.* **2013**, *135*, 1015–1025.
- (22) Dutta, S.; Chowdhury, G.; Gates, K. S. *J. Am. Chem. Soc.* **2007**, *129*, 1852–1853.
- (23) Price, N. E.; Johnson, K. M.; Wang, J.; Fekry, M. I.; Wang, Y.; Gates, K. S. *J. Am. Chem. Soc.* **2014**, *136*, 3483–3490.
- (24) Guillet, M.; Bioteux, S. *Mol. Cell. Biol.* **2003**, *23*, 8386–8394.
- (25) Gates, K. S.; Noonan, T.; Dutta, S. *Chem. Res. Toxicol.* **2004**, *17*, 839–856.
- (26) Gates, K. S. *Chem. Res. Toxicol.* **2009**, *22*, 1747–1760.
- (27) De Bont, R.; van Larebeke, N. *Mutagenesis* **2004**, *19*, 169–185.
- (28) Dong, M.; Wang, C.; Deen, W. M.; Dedon, P. C. *Chem. Res. Toxicol.* **2003**, *16*, 1044–1055.
- (29) Dutta, S.; Abe, H.; Aoyagi, S.; Kibayashi, C.; Gates, K. S. *J. Am. Chem. Soc.* **2005**, *127*, 15004–15005.
- (30) Fekry, M. I.; Price, N.; Zang, H.; Huang, C.; Harmata, M.; Brown, P.; Daniels, J. S.; Gates, K. S. *Chem. Res. Toxicol.* **2011**, *24*, 217–228.
- (31) Noonan, T.; Dutta, S.; Gates, K. S. *Chem. Res. Toxicol.* **2004**, *17*, 942–949.
- (32) Shipova, K.; Gates, K. S. *Bioorg. Med. Chem. Lett.* **2005**, *15*, 2111–2113.
- (33) Zang, H.; Gates, K. S. *Chem. Res. Toxicol.* **2003**, *16*, 1539–1546.
- (34) Fekry, M.; Szekely, J.; Dutta, S.; Breydo, L.; Zang, H.; Gates, K. S. *J. Am. Chem. Soc.* **2011**, *132*, 17641–17651.
- (35) Wilde, J. A.; Bolton, P. H.; Mazumdar, A.; Manoharan, M.; Gerlt, J. A. *J. Am. Chem. Soc.* **1989**, *111*, 1894–1896.
- (36) Muniandy, P. A.; Liu, J.; Majumdar, A.; Liu, S.-t.; Seidman, M. M. *Crit. Rev. Biochem. Mol. Biol.* **2010**, *45*, 23–49.
- (37) Schärer, O. D. *ChemBioChem.* **2005**, *6*, 27–32.
- (38) Shen, X.; Li, L. *Environ. Mol. Mutagen.* **2010**, *51*, 493–499.
- (39) Noll, D. M.; Mason, T. M.; Miller, P. S. *Chem. Rev.* **2006**, *106*, 277–301.
- (40) Clauson, C.; Schärer, O. D.; Niedernhofer, L. J. *Cold Spring Harbor Perspect. Biol.* **2013**, *5*, No. a012732.
- (41) Sturla, S. J. *Curr. Opin. Chem. Biol.* **2007**, *11*, 293–299.
- (42) Woo, J.; Sigurdsson, S. T.; Hopkins, P. B. *J. Am. Chem. Soc.* **1993**, *115*, 3407–3415.
- (43) Golankiewicz, B.; Ostrowski, T.; Leonard, P.; Seela, F. *Helv. Chim. Acta* **2002**, *85*, 388–398.
- (44) Gambino, J.; Yang, T.-F.; Wright, G. E. *Tetrahedron* **1994**, *50*, 11363–11368.
- (45) Espenson, J. H. *Chemical Kinetics and Reaction Mechanisms*, 2nd ed.; McGraw-Hill, Inc.: New York, 1995.
- (46) Liu, S.; Wang, J.; Su, Y.; Guerrero, C.; Zeng, Y.; Mitra, D.; Brooks, P. J.; Fisher, D. E.; Song, H.; Wang, Y. *Nucleic Acids Res.* **2013**, *41*, 6421–6429.
- (47) Riggins, J. N.; Daniels, J. S.; Rouzer, C. A.; Marnett, L. J. *J. Am. Chem. Soc.* **2004**, *126*, 8237–8243.
- (48) Hermida, S. A. S.; Possari, E. P. M.; Souza, D. B.; de Arruda Campos, I. P.; Gomes, O. F.; Di Mascio, P.; Medeiros, M. H. G.; Loureiro, A. P. M. *Chem. Res. Toxicol.* **2006**, *19*, 927–936.
- (49) Mons, S.; Fleet, G. W. J. *Org. Biomol. Chem.* **2003**, *1*, 3685–3691.
- (50) Takamura-Enya, T.; Watanabe, M.; Totsuka, Y.; Kanazawa, T.; Matsushima-Hibya, Y.; Koyama, K.; Sugimura, T.; Wakabayashi, K. *Proc. Natl. Acad. Sci. U.S.A.* **2001**, *98*, 12414–12419.
- (51) Hou, X.; Wang, G.; Gaffney, B. L.; Jones, R. A. *Nucleosides Nucleotides* **2009**, *28*, 1076–1094.
- (52) Narukulla, R.; Shuker, D. E. G.; Ramesh, V.; Xu, Y.-Z. *Magn. Reson. Chem.* **2008**, *46*, 1–8.
- (53) Christov, P. P.; Brown, K. L.; Kozekov, I. D.; Stone, M. P.; Harris, T. M.; Rizzo, C. J. *Chem. Res. Toxicol.* **2008**, *21*, 2324–2333.
- (54) Tomasz, M.; Lipman, R.; Lee, M. S.; Verdine, G. L.; Nakanishi, K. *Biochemistry* **1987**, *26*, 2010–2027.
- (55) Berger, M.; Cadet, J. Z. *Naturforsch.* **1985**, *40B*, 1519–31.
- (56) Cortes, S. J.; Mega, T. L.; Van Etten, R. L. *J. Org. Chem.* **1991**, *56*, 943–947.
- (57) Amann, N.; Wagenknecht, H.-A. *Tetrahedron Lett.* **2003**, *44*, 1685–1690.
- (58) Singh, M. P.; Hill, G. C.; Péoc'h, D.; Rayner, B.; Imbach, J.-L.; Lown, J. W. *Biochemistry* **1994**, *33*, 10271–10285.
- (59) Veldhuyzen, W. F.; Lam, Y.-F.; Rokita, S. E. *Chem. Res. Toxicol.* **2001**, *14*, 1345–1351.
- (60) Synold, T.; Xi, B.; Wuenschell, G. E.; Tamae, D.; Figarola, J. L.; Rahbar, S.; Termini, J. *Chem. Res. Toxicol.* **2008**, *21*, 2148–2155.
- (61) Cordes, E. H.; Jencks, W. P. *J. Am. Chem. Soc.* **1963**, *85*, 2843–2848.
- (62) Holton, S.; Runquist, O. *J. Org. Chem.* **1961**, *26*, 5193–5195.
- (63) Wang, Y.; Wang, Y. *Anal. Chem.* **2003**, *75*, 6306–6313.
- (64) Cao, H.; Hearst, J. E.; Corash, L.; Wang, Y. *Anal. Chem.* **2008**, *80*, 2932–2938.
- (65) Lai, C.; Cao, H.; Hearst, J. E.; Corash, L.; Luo, H.; Wang, Y. *Anal. Chem.* **2008**, *80*, 8790–8798.
- (66) Mao, H.; Schnetz-Boutaud, N. C.; Weisenseel, J. P.; Marnett, L. J.; Stone, M. P. *Proc. Natl. Acad. Sci. U.S.A.* **1999**, *96*, 6615–6620.
- (67) Adrover, M.; Vilanova, B.; Muñoz, F.; Donoso, J. *Bioorg. Chem.* **2009**, *37*, 26–32.
- (68) Caldés, C.; Vilanova, B.; Adrover, M.; Muñoz, F.; Donoso, J. *Chem. Biodiversity* **2011**, *8*, 1318–1332.
- (69) Capon, B.; Connett, B. E. *J. Chem. Soc.* **1965**, 4497–4502.
- (70) Bridiau, N.; Benamansour, M.; Legoy, M. D.; Maugard, T. *Tetrahedron* **2007**, *63*, 4178–4183.
- (71) Na, Y.; Shen, H.; Byers, L. D. *Bioorg. Chem.* **2011**, *39*, 111–113.
- (72) Sianipar, A.; Parkin, J. E.; Sunderland, V. B. *Int. J. Pharm.* **1998**, *176*, 55–61.
- (73) Cordes, E. H.; Jencks, W. P. *J. Am. Chem. Soc.* **1962**, *84*, 832–837.